



弗拉—法门转折期气候—海洋环境变化及生物危机成因探讨

张力钰, 陈代钊, 刘康

引用本文:

张力钰, 陈代钊, 刘康. 弗拉—法门转折期气候—海洋环境变化及生物危机成因探讨[J]. 沉积学报, 2024, 42(3): 723–737.
ZHANG LiYu, CHEN DaiZhao, LIU Kang. Paleoclimatic and Paleo-Oceanic Environment Evolution in the Frasnian–Famennian Transition: Potential causes of the biotic crisis[J]. *Acta Sedimentologica Sinica*, 2024, 42(3): 723–737.

相似文章推荐（请使用火狐或IE浏览器查看文章）

Similar articles recommended (Please use Firefox or IE to view the article)

峡东地区震旦纪最早期风暴沉积记录及其地质意义

Early Sinian Storm Deposits in the Eastern Yangtze Gorges Area and their Geological Significance
沉积学报. 2020, 38(1): 182–195 <https://doi.org/10.14027/j.issn.1000-0550.2019.003>

火山灰沉积与页岩有机质富集关系探讨——以五峰组—龙马溪组含气页岩为例

Discussion of the Relationship between Volcanic Ash Layers and Organic Enrichment of Black Shale: A case study of the Wufeng–Longmaxi gas shales in the Sichuan Basin
沉积学报. 2019, 37(6): 1296–1308 <https://doi.org/10.14027/j.issn.1000-0550.2019.088>

赫南特冰期古海洋环境转变及其成因机制研究现状

The Genesis of Hirnantian Glaciation and Paleo–Ocean Environment During Ordovician–Silurian Transition
沉积学报. 2018, 36(2): 319–332 <https://doi.org/10.14027/j.issn.1000-0550.2018.037>

扬子地区中—晚奥陶世转折期的碳同位素漂移事件及其成因探讨

Carbon Isotope Excursions Near the Middle–Late Ordovician Transition in the Yangtze Area and Their Possible Genesis
沉积学报. 2016, 34(6): 1021–1031 <https://doi.org/10.14027/j.cnki.cjxb.2016.06.002>

南雄盆地晚白垩世—古新世陆源沉积组份变化的古气候指示

Paleoclimate Indication of Terrigenous Clastic Rock's Component during the Late Cretaceous–Early Paleocene in the Nanxiong Basin
沉积学报. 2015, 33(1): 116–123 <https://doi.org/10.14027/j.cnki.cjxb.2015.01.012>

文章编号:1000-0550(2024)03-0723-15

DOI: 10.14027/j.issn.1000-0550.2023.107

弗拉—法门转折期气候—海洋环境变化及生物危机成因探讨

张力钰^{1,2},陈代钊³,刘康⁴

1.中国石化石油勘探开发研究院,无锡石油地质研究所,江苏无锡 214126

2.中国石化油气成藏重点实验室,江苏无锡 214126

3.中国科学院地质与地球物理研究所,新生代地质与环境院重点实验室,北京 100029

4.中国石油勘探开发研究院,油气地球化学重点实验室,北京 100083

摘要 【目的】晚泥盆世弗拉—法门(Frasnian-Famennian, F-F)转折期是地质历史的一个关键时期,海洋生态系统发生了重大变化并造成了低纬度地区浅海底栖生物的大量灭绝。关于该时期的古气候、古海洋环境变化以及生物灭绝的成因机制研究目前已取得一定的进展,但仍然存在争议且各环境要素之间的相互作用尚不明确。【方法】在系统梳理F-F转折期古气候、古海洋环境变化研究现状的基础上,结合华南的研究实例探讨了F-F转折期的古海洋缺氧模式。【结果与结论】F-F转折期,气候在变冷的趋势下出现多次快速的暖—冷交替;缺氧范围和程度各地表现不一,但主要集中在低纬度浅海地区上Kellwasser层附近。因此,F-F生物危机并不是单一因素造成的。频繁、短暂的火山活动引起大陆风化作用增强,一方面导致了气候快速的暖—冷交替,另一方面促进了陆地向海洋中输入营养物质造成浅海的富营养化和缺氧。各个环境因素相互制约/影响对低纬度浅海地区生命造成极大的环境压力,最终导致了F-F生物危机。

关键词 弗拉—法门转折期;古气候;古海洋氧化还原状态;生物危机

第一作者简介 张力钰,女,1992年出生,博士,助理研究员,沉积学与沉积地球化学,E-mail: zhangliyu.syky@sinopec.com

中图分类号 P512.2 文献标志码 A

0 引言

泥盆纪晚期是地质历史关键时期,地球表生系统发生了显著变化,期间发生了诸如维管束植物登陆^[1]、大陆风化作用增强^[2-3]、全球气候由温室转变为冰室^[4-6]、火山活动^[7-9]、生物灭绝等重大地质事件^[10-14]。其中,以晚泥盆世弗拉—法门(Frasnian-Famennian, F-F)转折期的生物灭绝事件最为显著,被称为F-F事件或者Kellwasser事件(可细分为上Kellwasser事件和下Kellwasser事件,分别位于牙形刺 *Pamatolepis rhenana* 带下部和 *Pamatolepis linguiformis* 带顶部),也被认定为显生宙五大生物集群灭绝事件之一^[15-18]。

F-F生物灭绝事件实际上是一次循序的、渐进式生物灭亡的结果,从中泥盆世拉开序幕,在F-F界线附近达到顶峰(主幕)^[19]。此次事件造成约21%科,50%属和80%种发生了灭绝^[10,20],其中低纬度浅海底栖生物受到的影响最大,高纬度、深海生物和陆地生

物所受影响甚微^[18,21]。泥盆纪典型的珊瑚—孔虫礁几乎全部消亡,世界范围内,47个浅水型四射珊瑚属仅2~3个属残存下来,而151个种的珊瑚几乎全部灭绝^[19,22-23]。层孔虫属的数量急剧减少,35个属中24个属灭绝,灭绝率高达68%^[24-25];腕足动物也受到重创,五房贝目和无洞贝目灭绝,正形贝目和扭月贝目受到重创,71个弗拉期的属仅10属存活下来,损失率约为86%,继之以法门期长身贝目、石燕贝目和小嘴贝目繁盛为特征^[25];三叶虫5个目中3个目消失,6个科的分子消失,目一级灭绝率达60%^[25];浅海底介形类世界各地灭绝强度有所差异,种一级的灭绝率介于65%~80%^[26],深水介形类受影响较弱;大量弗拉期典型牙形刺分子消亡,全球范围内弗拉阶顶部的 *Pamatolepid* 生物相、*Pamatolepid-Polygnathid* 生物相转变为法门阶底部的 *Pamatolepid-Icriodid* 生物相^[27]。竹节石几乎全部灭绝,25个属仅有3个属的个别分子延续至法门期早期^[28];菊石约67%的属,88%

的种灭绝^[29]。深水放射虫影响很小，并在灭绝事件之后有上升的趋势^[21]。

关于此次生物危机的成因机制，大量学者通过沉积学、地球化学等手段进行了探讨，主要包括海平面变化^[30-31]、海洋缺氧及富营养化^[32-36]、气候变化^[27,37-38]、火山(热液)活动^[8-9]以及地外事件^[12,39]等。通过Web of Science以Late Devonian mass extinction(晚泥盆生物灭绝)和Frasnian-Famennian(弗拉—法门转折期)为关键词检索了2000—2023年文献，显示气候变化和海洋缺氧是目前认可度和讨论度(被引率)最高的假说，且越来越多的证据表明各环境要素之间相互影响与制约。在F-F转折期，古气候与古海洋环境具备怎样的特征，不同环境要素之间如何协同变化，以及导致F-F生物危机的最核心因素是什么，都是值得总结和探讨的科学问题，也对理解这一时期地球环境—生命协同演化规律具有重要意义。

拟通过对F-F转折期气候、古海洋环境变化的研究现状进行系统梳理，并结合华南的最新研究成果，详细论述F-F转折期的古气候演化规律、古海洋氧化还原结构以及最可能的生物灭绝机制，以期为下一步的研究提供思路。

1 晚泥盆世全球古地理与F-F事件主要研究区

晚泥盆世古地理的基本格局主要由冈瓦纳古

陆、劳伦西亚大陆及其间的古特提斯洋、泛大洋组成。劳伦西亚大陆以东由一些分散的大型陆块或小型至微型陆地群组成，其中，以西伯利亚、哈萨克斯坦、中国华北和华南古陆较大。冈瓦纳大陆主体位于30°S以南，劳伦西亚大陆、华南板块、华北板块、塔里木板块和哈萨克斯坦板块主体位于赤道附近(南北纬30°之间)(图1)。劳伦西亚大陆中央为南北向的加里东造山带隆起区，东西两侧发育广阔陆表海。冈瓦纳古陆为广大隆起区，北缘发育宽阔陆表海。劳伦西亚大陆东南缘与冈瓦纳大陆西北缘之间以狭窄的瑞亚克洋相隔。华南板块由华夏和扬子地块拼合而成，主体为隆升剥蚀区，周缘主要为陆表海^[40]。

全球范围内，F-F事件的研究区主要集中在瑞亚克洋周缘水体受限的构造盆地、华力西—阿拉契亚一带的陆表盆地、陆缘盆地和华南的沉积盆地中，主要包括当时低纬度地区的欧洲各地、北美东部和华南地区，研究内容包括古生物、沉积学、地层学、地球化学等方面^[25](图1)。

拉利剖面位于广西壮族自治区宜州市，上泥盆统由老至新可划分为老爷坟组、香田组和五指山组。老爷坟组以灰色中厚层生屑灰岩、砂屑灰岩为主，香田组以浅灰—深灰中薄层泥晶灰岩，泥质条带灰岩和扁豆状灰岩为主，五指山组主要为深灰色薄层—中层瘤状灰岩、扁豆状灰岩。针对不同岩性系统采集了拉利F-F界线剖面新鲜岩样，对其中55件样品进行了碳氧同位素分析，19件样品进行了稀土元素分析。碳氧

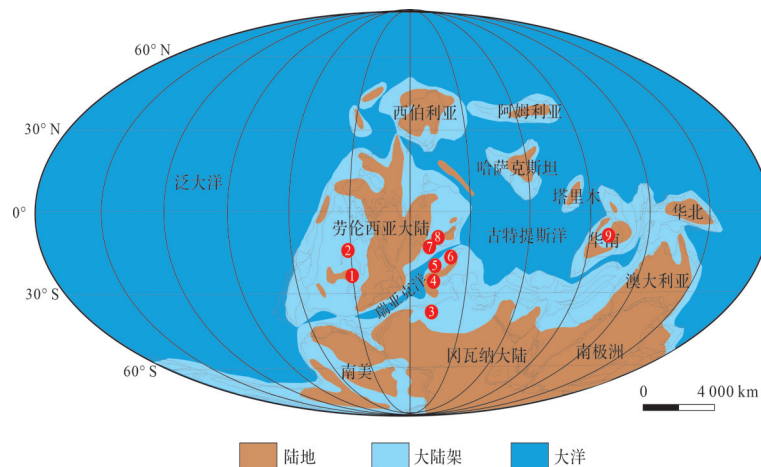


图1 晚泥盆世全球古地理图和F-F事件主要研究区(据文献[38]修改)

F-F事件主要研究地点：1.美国；2.加拿大；3.摩洛哥；4.西班牙；5.法国；6.奥地利；7.德国；8.波兰；9.中国

Fig.1 Global paleogeographic map and main study areas of Frasnian-Famennian (F-F) events in the Late Devonian
(modified from reference [38])

main research sites for F-F events: 1. USA; 2. Canada; 3. Morocco; 4. Spain; 5. France; 6. Austria; 7. Germany; 8. Poland; 9. China

同位素与稀土元素分析分别在中国科学院地质与地球物理研究所(IGGCAS)稳定同位素地球化学实验室和成矿年代学实验室完成。碳同位素和氧同位素的精度分别高于 0.20‰ 和 0.15‰ 。稀土元素测试误差小于10%。

2 弗拉—法门转折期气候变化

每种生物都有其最适宜的生存温度区间,小幅度的气温变化也可能对F-F事件中受影响最甚的低纬度(南北纬 30° 之间)浅海底栖生物种群产生致命的打击。F-F转折期,气候变暖和变冷的假说都有支持者。早期有学者提出F-F之交的海水温度可达 40°C ,温度的升高可能造成F-F生物危机^[41]。然而更多证据表明弗拉晚期温度较高,存在一个“温室”气候,F-F转折期,气候变冷,逐渐向“冰室”转化^[4,37,42]。

Strel et al.^[4]根据孢粉组合的分类多样性研究,认为吉维特期和弗拉期温度较高并在弗拉末期达到最高;法门早期,孢粉多样性下降,表明F-F转折期气候变冷。北美(加拿大)、华南(广西)在F-F界线之下发育的因海平面下降造成的碳酸盐台地暴露/岩溶作用^[4,33,43]亦被认为是F-F转折期气候变冷的重要证据。此外,氧、碳、锶等同位素更为精细地刻画了F-F转折期的气候变化。

Joachimski et al.^[37]对德国 Rheinische Schiefergebirge地区的两条F-F界线剖面进行了牙形刺氧同位素($\delta^{18}\text{O}_{\text{PO}_4}$)分析,结果显示上、下Kellwasser层(Upper/Lower Kellwasser Horizons, 即UKH和LKH) $\delta^{18}\text{O}_{\text{PO}_4}$ 值出现了 $+1\text{‰} \sim +1.5\text{‰}$ (VSMOW)的正偏移,由此计算出F-F转折期海水温度大致下降了 $5^{\circ}\text{C} \sim 7^{\circ}\text{C}$ 。之后,他又分析了欧洲、北美、澳大利亚的多条泥盆纪剖面的牙形刺氧同位素,结果表明,从早泥盆世的布拉格期(Pragian)到中泥盆世的吉维特(Givetian)中期,温度逐渐从 30°C 下降至 22°C ;从吉维特(Givetian)中期到晚泥盆世的弗拉(Frasnian)晚期,温度又逐渐上升至 30°C ;在弗拉期和法门期之交,温度小幅降低^[6]。类似地,Le Houedec et al.^[44]使用牙形刺氧同位素温度计在法国和摩洛哥的F-F界线剖面中也识别到弗拉期和法门期之交的小幅降温事件。由于欧洲、北美等地很多深水F-F界线剖面高度凝缩^[45-46],高分辨率的地球化学和环境信号可能存在缺失或叠加,华南F-F剖面一般是欧洲同期剖面厚度的2~5倍,沉积速率适中,能更好地保存当时的海洋环

境信息。Huang et al.^[27]和Zhang et al.^[47]对华南的付合(杨堤)和拉利F-F界线剖面进行了高精度的牙形刺氧同位素分析,结果显示F-F之交海水温度变化范围为 $27^{\circ}\text{C} \sim 36^{\circ}\text{C}$,与欧美地区接近,LKH-UKH存在明显的快速降温事件。特别地,付合(杨堤)剖面海水温度在F-F转折期有多次短周期的暖—冷交替波动,而非单调下降。

除氧同位素外,碳($\delta^{13}\text{C}$)和锶同位素($^{87}\text{Sr}/^{86}\text{Sr}$)也是极好的古气候指标。F-F事件中, $\delta^{13}\text{C}$ 值在UKH-LKH出现了全球性的碳同位素正偏移,幅度 $+2\text{‰} \sim +4\text{‰}$ ^[48-49],此次正偏移一般被认为是有机碳快速埋藏的结果,伴随着全球大气 CO_2 分压($p\text{CO}_2$)的下降和气候的变冷^[19,48-50]。此外,有研究认为碳酸盐岩的无机碳(C_{carb})和有机碳(C_{org})同位素差值 $\delta^{13}\text{C}_{\text{carb-org}}$ 不仅仅代表了不同碳库中初始同位素组成,更代表了固定 CO_2 过程中初级生产者(浮游植物)与海水溶解的 CO_2 以及 $p\text{CO}_2$ 之间的碳同位素分馏效应(ϵ_p)。当 $p\text{CO}_2$ 升高时(气温升高)时,分馏作用增强, $\delta^{13}\text{C}_{\text{carb-org}}$ 值升高,反之亦然^[48,51-54]。华南付合(杨堤)剖面碳同位素结果显示F-F之交 $\delta^{13}\text{C}_{\text{carb-org}}$ 整体下降,且中间存在3次明显的波动旋回^[8],波动趋势与该剖面的 $\delta^{18}\text{O}_{\text{PO}_4}$ 结果刚好相反^[38](图2),进一步证实了F-F转折期的气候在整体变冷的趋势下存在多期暖—冷交替。因此,气候的整体变冷与风化作用的长期效应和有机碳快速埋藏有关。

海水的锶同位素组成($^{87}\text{Sr}/^{86}\text{Sr}_{\text{sw}}$)主要由“壳源锶”和“幔源锶”的相对输入量及其同位素比值决定^[55-56]。全球海水 $^{87}\text{Sr}/^{86}\text{Sr}$ 值曲线显示从中泥盆世吉维特晚期到晚泥盆世弗拉早期,海水 $^{87}\text{Sr}/^{86}\text{Sr}$ 值呈上升趋势,这可能是Eovariscan造山运动引起的地壳抬升和大陆风化作用增强导致^[2,57]。此外,Algeo et al.^[58]提出中泥盆世维管束植物向陆的快速扩张可能引起硅酸盐风化作用增强。然而,这种长周期的风化作用增强是无法解释F-F转折期的气候快速变化的。Zhang et al.^[38]对F-F转折期华南付合剖面和波兰Kowala剖面进行了高精度的牙形刺 $^{87}\text{Sr}/^{86}\text{Sr}$ 值分析,在F-F转折期发现了三次明显的 $^{87}\text{Sr}/^{86}\text{Sr}$ 值波动(特别是付合剖面,图2中阶段I,II,III),每次波动(~200 kyr)对应着 $^{87}\text{Sr}/^{86}\text{Sr}$ 值从小(负偏移)到大(正偏移)的变化,且与碳—氧同位素有着极好的对应关系: $^{87}\text{Sr}/^{86}\text{Sr}$ 值降低(负偏移)时, $\delta^{13}\text{C}_{\text{carb-org}}$ 增大(正偏移), $\delta^{18}\text{O}_{\text{PO}_4}$ 减小(负偏移),反之亦然(图2)。对此,Zhang

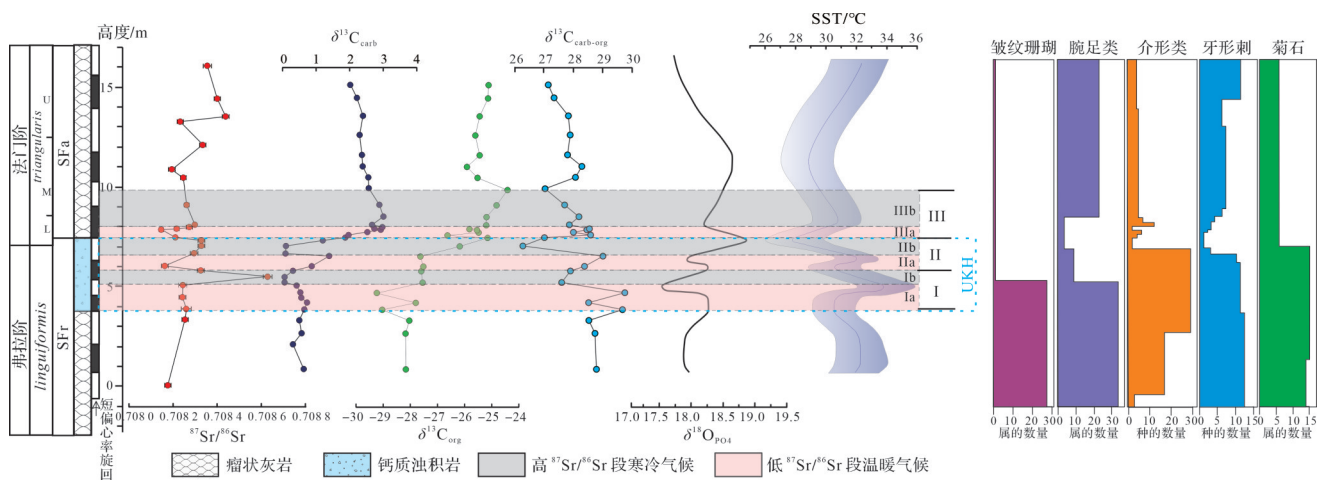


图2 付合剖面F-F转折期 $^{87}\text{Sr}/^{86}\text{Sr}$, $\delta^{13}\text{C}_{\text{carb}}$, $\delta^{13}\text{C}_{\text{org}}$, $\delta^{13}\text{C}_{\text{carb-org}}$, $\delta^{18}\text{O}_{\text{PO}_4}$ 和表层海水温度(SST)数据与生物多样性对比图(据文献[27,38]修改)

牙形刺 $^{87}\text{Sr}/^{86}\text{Sr}$ 值引自文献[38];全岩 $\delta^{13}\text{C}_{\text{carb}}$, $\delta^{13}\text{C}_{\text{org}}$ 和 $\delta^{13}\text{C}_{\text{carb-org}}$ 数据引自文献[8]; $\delta^{18}\text{O}_{\text{PO}_4}$ 和SST数据、古生物数据引自文献[27];SFa, SFr层序及旋回划分引自文献[13];阶段I, II, III代表F-F转折期三次明显的 $^{87}\text{Sr}/^{86}\text{Sr}$ 值波动,阶段I和II大致与UKH层对应

Fig.2 Comparison of biodiversity and $^{87}\text{Sr}/^{86}\text{Sr}$, $\delta^{13}\text{C}_{\text{carb}}$, $\delta^{13}\text{C}_{\text{org}}$, $\delta^{13}\text{C}_{\text{carb-org}}$, $\delta^{18}\text{O}_{\text{PO}_4}$ and sea-surface temperature (SST) data at Fuhe section during F-F transition (modified from references [27,38])

conodont $^{87}\text{Sr}/^{86}\text{Sr}$ data from reference [38]; bulk-rock $\delta^{13}\text{C}_{\text{carb}}$, $\delta^{13}\text{C}_{\text{org}}$ and $\delta^{13}\text{C}_{\text{carb-org}}$ data from reference [8]; $\delta^{18}\text{O}_{\text{PO}_4}$, SST and paleontological data from reference [27]; sequence and cycle division of SFa and SFr from reference [13]; intervals I, II, III represent three distinct Sr isotope fluctuations during F-F transition (intervals I and II roughly correspond to UKH layer)

et al.^[38]认为小规模的火山放气作用会向大气中释放大量温室气体,气候变暖,水循环加速, $\delta^{13}\text{C}_{\text{carb-org}}$ 值增大, $\delta^{18}\text{O}_{\text{PO}_4}$ 值减小,陆地风化作用增强,引起陆源锶通过河流输入至海洋, $^{87}\text{Sr}/^{86}\text{Sr}$ 值增大;随着风化作用消耗掉大气CO₂,pCO₂降低,气候逐渐变冷, $\delta^{13}\text{C}_{\text{carb-org}}$ 值变小, $\delta^{18}\text{O}_{\text{PO}_4}$ 值增大, $^{87}\text{Sr}/^{86}\text{Sr}$ 值减小。因此,间歇性、短周期的火山放气作用引起的风化作用变化和气候暖—冷交替导致了F-F转折期频繁的C-O-Sr同位素变化。

综上所述,中泥盆吉维特晚期—晚泥盆世弗拉晚期,气候逐渐升温;弗拉末期,温度达到最高;弗拉末期—法门早期(F-F转折期),气候整体变冷,但中间存在多次暖—冷交替。频繁、短周期的火山放气作用引起的风化作用变化可能是该时期气候暖—冷交替的根本原因。

3 弗拉—法门转折期古海洋缺氧状况

氧气是生物赖以生存的基本条件,从地球出现原始生命后,生物经历了从简单到复杂、从低等到高等、从水生到陆生的演化,这都与大气和海洋氧含量的增长密不可分。大多数F-F界线剖面的UKH,LKH层以特征性的沥青质灰岩和黑色页岩沉积为主^[33,59-60],因此

海洋缺氧导致了F-F生物危机的假说经久不衰。

3.1 全球海水氧化还原状态

欧洲、北美地区的多条F-F界线剖面在UKH层识别到粒径较小且变化范围狭窄的草莓状黄铁矿,指示了UKH层的缺氧事件,但LKH层缺氧信号较弱^[33,61]。Mn-Mo-U-V等氧化还原敏感元素在部分欧洲、北美剖面的UKH和LKH层有较明显的富集,指示了缺氧事件的存在^[35,60]。Haddad *et al.*^[62]对北美Appalachian盆地UKH层的高分辨率微量元素分析认为UKH层内的缺氧是间歇性存在,并非持续缺氧。此外,氮同位素($\delta^{15}\text{N}_{\text{org}}$)在Kellwasser层的正偏移^[35]、碳酸盐晶格硫酸盐和黄铁矿的硫同位素(S_{CAS}, S_{Py})在UKH的波动^[8,63],营厌氧光合作用的绿硫细菌生物标志化合物的出现^[34,64]均证实了Kellwasser缺氧事件,特别是在UKH层,有明显的缺氧甚至硫化。

然而,绝大多数的研究剖面都出现在特定的环境中,特别是靠近物源的陆表海、陆缘海盆地^[65]。相反,部分离岸的、高纬度地区的F-F剖面中则缺乏明显缺氧记录^[66-67]。此外,以上指标大多仅代表了局部或者区域性的缺氧事件,对全球性海水缺氧的指示意义不强。

近年来,U同位素($\delta^{238}\text{U}$)不断被用于全球海洋缺氧面积的定量研究^[68-70]。学者对来自美国内华达

Devil's Gate 组^[36]和我国广西白沙剖面^[71]的碳酸盐岩进行了 $\delta^{238}\text{U}$ 分析,结果显示 UKH 和 LKH 层附近(与 UKH、LKH 层不完全对应)均出现了 $\delta^{238}\text{U}$ 负偏移,并由此(根据质量平衡模型)计算出全球海洋底层水体的缺氧面积增加了 5%~15%,且总体海洋缺氧面积小于 20%。White *et al.*^[36]同时指出,缺氧海水主要集中在亚热带地区的陆缘海 UKH 和 LKH 层,缺氧面积分别为~45%(LKH)和~79%(UKH);但缺氧事件不仅仅

局限于 Kellwasser 层,延伸范围可能更广(例如从牙形刺 *Hassi* 带到 *Crepida* 带均出现),且各研究剖面之间的缺氧程度和出现位置差异较大(图 3)。不难看出,F-F 转折期的海洋缺氧事件在一定程度上是“局限”的,主要集中在低纬度靠近陆源的陆表海/陆缘海,深海则不缺氧。缺氧事件在 UKH 层达到顶峰,但在 UKH 层内仍然是间歇性缺氧;LKH 层缺氧信号较弱,以次氧—氧化为主。

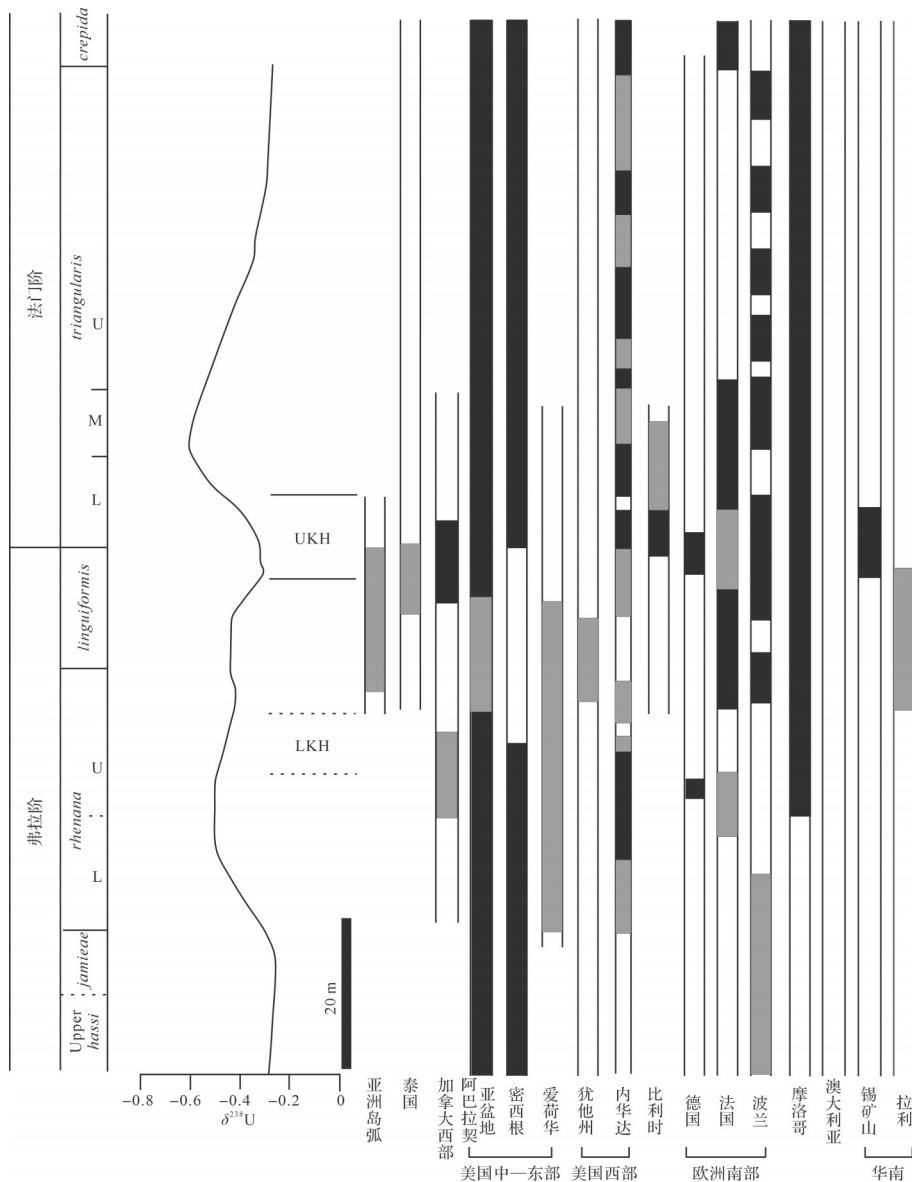


图 3 晚泥盆世全球不同地区海水缺氧状况对比图(据文献[36]修改)

锡矿山剖面数据引自文献[72],拉利剖面数据来自本文, $\delta^{238}\text{U}$ 数据和其余地区海水缺氧状况引自文献[36],黑色框代表缺氧,灰色框代表次氧—间歇性缺氧

Fig.3 Comparison of marine anoxia in different regions of the Earth in the Late Devonian
(modified from reference [36])

Xikuangshan section data from reference [72]; Lali section data from this paper, $\delta^{238}\text{U}$ and marine anoxia data in other areas from reference [36]; black boxes, anoxia; gray boxes, sub-anoxia/intermittent anoxia

3.2 华南地区海水氧化还原状态和缺氧模式

针对 Kellwasser 缺氧事件, 目前有两种模型: (1)“由下至上型”, 即深层缺氧水体的上涌引起缺氧; (2)“由上至下型”, 即大陆风化作用增强向海洋输入大量营养物质, 导致富营养化和缺氧^[33,35,65,73]。

3.2.1 拉利剖面氧化还原状态

拉利剖面的碳酸盐岩碳氧同位素 ($\delta^{13}\text{C}_{\text{carb}}$, $\delta^{18}\text{O}_{\text{carb}}$) 和稀土元素分析结果详见表 1 和表 2。 $\delta^{13}\text{C}_{\text{carb}}$ 值介于 $+0.99\text{\textperthousand}$ ~ $+3.53\text{\textperthousand}$ (VPDB)。 $\delta^{18}\text{O}_{\text{carb}}$ 值介于 $-1.45\text{\textperthousand}$ ~ $-6.37\text{\textperthousand}$ (VPDB), 平均值为 $-4.19\text{\textperthousand}$ VPDB ($n=55$)。垂向上, 碳同位素发生了两次明显的正偏移。第一次正偏移发生在香田组底部, LKH 层附近, $\delta^{13}\text{C}_{\text{carb}}$ 值由 $1.06\text{\textperthousand}$ (LL-41) 增长到 $3.53\text{\textperthousand}$ (LL-46), 增幅 $2.22\text{\textperthousand}$ 。第二次正偏移发生在 F-F 界线附近, 即 UKH 层, $\delta^{13}\text{C}_{\text{carb}}$ 值由 $0.28\text{\textperthousand}$ (LL-68) 增长到 $3.17\text{\textperthousand}$ (LL-77), 增幅为 $2.89\text{\textperthousand}$ 。Y/Ho 比值介于 $33.48\text{--}54.42$, 平均值为 42.34 ($n=19$)。Ce/Ce* ($\text{Ce}/\text{Ce}^* = \text{Ce}/(\text{La} + \text{Pr})$) 值介于 $0.13\text{--}0.73$, 变化范围较大, 平均值为 0.53 ($n=19$)。

Y/Ho 比值被广泛用于指示陆源输入量, 后太古宙澳大利亚页岩 (Post-Archean Australian Shale, PAAS) 和现代海水的 Y/Ho 比值分别为 ~ 27 和 ~ 44 ^[74-75], 拉利剖面 19 个灰岩样品的 Y/Ho 平均值为 42.34 , 接近现代海水值, 表明陆源碎屑混入量很少。此外, 海相碳酸盐岩 $\delta^{18}\text{O}_{\text{carb}}$ 大于 $-5\text{\textperthousand}$ 时, 一般认为其基本不受成岩流体改造^[76]。拉利剖面的除极个别样品 $\delta^{18}\text{O}_{\text{carb}}$ 大于 $-5\text{\textperthousand}$ 外, 其余样品的 $\delta^{18}\text{O}_{\text{carb}}$ 值均小于 $-5\text{\textperthousand}$, 且 $\delta^{13}\text{C}_{\text{carb}}$ 与 $\delta^{18}\text{O}_{\text{carb}}$ 之间相关性很低 ($R^2=0.03$, 图 4), 说明拉利剖面的灰岩样品受成岩作用影响较小, 较好地记录了当时的海水信号。

现代海洋中, Ce^{3+} 容易被锰 (Mn) 的氧化物或者细菌等氧化成 Ce^{4+} 。 Ce^{4+} 容易吸附在 Mn 氧化物或者氢氧化物的表面, 从海水中清除。因此, 相对于其他 +3 价的稀土元素 (Rare Earth Element, REE), Ce 在海水中的溶解度变低, 导致氧化的海水亏损 Ce, 呈现 Ce 负异常; 缺氧的海水 Ce/Ce^* 值相对较高^[77-78]。拉利剖面 Ce/Ce^* 值介于 $0.13\text{--}0.73$, 平均值为 0.53 。垂向上, Ce/Ce^* 值在香田组顶部 (F-F 界线之下) 瘤状

表 1 拉利剖面 $\delta^{13}\text{C}_{\text{carb}}$ 和 $\delta^{18}\text{O}_{\text{carb}}$ 数据表

Table 1 $\delta^{13}\text{C}_{\text{carb}}$ and $\delta^{18}\text{O}_{\text{carb}}$ data at Lali section

样品编号	高度/m	$\delta^{13}\text{C}_{\text{carb}}\text{\textperthousand}$	$\delta^{18}\text{O}_{\text{carb}}\text{\textperthousand}$	样品编号	高度/m	$\delta^{13}\text{C}_{\text{carb}}\text{\textperthousand}$	$\delta^{18}\text{O}_{\text{carb}}\text{\textperthousand}$	样品编号	高度/m	$\delta^{13}\text{C}_{\text{carb}}\text{\textperthousand}$	$\delta^{18}\text{O}_{\text{carb}}\text{\textperthousand}$
LL-33	1.40	2.48	-5.01	LL-52	17.20	1.37	-4.15	LL-71	29.15	1.82	-4.41
LL-34	2.50	2.94	-4.67	LL-53	18.10	1.28	-4.36	LL-72	29.75	2.53	-3.89
LL-35	3.50	1.98	-4.31	LL-54	18.60	1.36	-4.14	LL-73	30.05	2.04	-4.89
LL-36	4.50	2.19	-4.01	LL-55	19.05	1.37	-4.13	LL-74	30.30	3.07	-5.72
LL-37	5.60	2.68	-4.56	LL-56	19.70	1.37	-3.61	LL-75	30.50	2.98	-6.19
LL-38	6.50	2.45	-4.33	LL-57	20.25	1.27	-4.01	LL-76	31.15	2.85	-1.45
LL-39	7.40	2.67	-3.83	LL-58	20.90	1.18	-4.41	LL-77	31.75	3.17	-4.47
LL-40	8.80	2.34	-4.85	LL-59	21.55	1.12	-4.90	LL-78	32.40	2.45	-4.55
LL-41	8.95	1.31	-4.46	LL-60	22.30	1.10	-3.06	LL-79	32.70	1.71	-3.98
LL-42	9.75	2.37	-6.37	LL-61	23.00	1.12	-3.67	LL-80	33.35	1.89	-4.31
LL-43	10.55	2.58	-4.69	LL-62	24.70	1.04	-3.72	LL-81	34.10	1.76	-4.18
LL-44	11.25	3.01	-4.61	LL-63	24.40	1.04	-4.17	LL-82	35.00	1.53	-4.02
LL-45	11.65	2.28	-3.16	LL-64	25.00	1.09	-4.24	LL-83	35.70	1.52	-3.62
LL-46	12.35	3.53	-3.61	LL-65	25.60	1.00	-5.11	LL-84	37.00	1.28	-3.88
LL-47	12.85	1.53	-4.01	LL-66	26.10	0.99	-4.41	LL-85	38.20	1.43	-3.69
LL-48	13.90	1.54	-3.08	LL-67	26.55	1.18	-4.50	LL-86	39.90	1.19	-3.83
LL-49	14.60	2.63	-3.37	LL-68	27.25	1.06	-4.20	LL-87	40.80	1.09	-3.97
LL-50	15.60	1.72	-4.07	LL-69	27.90	—	—	LL-88	42.00	2.93	-4.02
LL-51	16.30	1.64	-4.04	LL-70	28.50	1.51	-3.40				

表2 拉利剖面稀土元素数据表
Table 2 REE data at Lali section

样品 编号	高度/m	La	Ce	Pr	Nd	Sm	Eu	Gd	Tb	Dy	Y	Ho	Er	Tm	Yb	Lu	Ce/Ce [*]	Y/Ho
		$\times 10^{-6}$																
LL-34	2.50	0.90	0.58	0.13	0.56	0.09	0.02	0.13	0.02	0.14	1.52	0.03	0.09	0.01	0.08	0.01	0.38	48.48
LL-36	4.50	2.30	1.64	0.35	1.46	0.26	0.06	0.32	0.05	0.34	3.19	0.07	0.20	0.03	0.19	0.03	0.41	43.38
LL-40	8.80	0.62	0.29	0.09	0.35	0.06	0.01	0.09	0.01	0.09	1.04	0.02	0.05	0.01	0.05	0.01	0.27	52.55
LL-46	12.35	3.04	2.41	0.60	2.51	0.49	0.09	0.49	0.08	0.50	4.08	0.11	0.29	0.04	0.26	0.04	0.41	38.55
LL-49	14.60	0.26	0.06	0.03	0.14	0.03	0.01	0.04	0	0.03	0.41	0.01	0.02	0	0.02	0	0.13	53.20
LL-52	17.20	4.38	5.17	0.72	3.21	0.60	0.13	0.74	0.11	0.66	5.43	0.14	0.39	0.05	0.32	0.06	0.66	37.70
LL-53	18.10																	
LL-54	18.60	7.44	9.56	1.20	4.69	0.84	0.22	1.03	0.17	1.06	8.72	0.23	0.65	0.09	0.62	0.11	0.72	37.58
LL-57	20.25	4.46	5.27	0.66	2.55	0.49	0.13	0.55	0.07	0.44	4.38	0.09	0.25	0.04	0.21	0.04	0.69	48.37
LL-60	22.30	3.48	3.73	0.45	1.86	0.35	0.08	0.44	0.07	0.54	4.87	0.13	0.38	0.06	0.36	0.06	0.65	38.40
LL-65	25.60	2.02	2.19	0.24	1.05	0.16	0.03	0.18	0.02	0.12	1.32	0.02	0.07	0.01	0.06	0.01	0.68	54.42
LL-68	27.25	0.87	1.09	0.13	0.49	0.09	0.02	0.10	0.01	0.09	0.77	0.02	0.06	0.01	0.05	0.01	0.73	39.47
LL-69	27.90	3.04	3.98	0.55	2.23	0.44	0.10	0.51	0.08	0.54	4.59	0.12	0.31	0.04	0.26	0.04	0.70	38.22
LL-70	28.50	2.73	3.50	0.53	2.16	0.38	0.08	0.44	0.07	0.45	3.39	0.10	0.26	0.04	0.23	0.04	0.66	34.76
LL-71	29.15	1.40	1.70	0.21	0.87	0.16	0.03	0.16	0.02	0.13	1.13	0.03	0.07	0.01	0.06	0.01	0.70	41.05
LL-74	30.30	1.61	1.50	0.25	0.97	0.18	0.03	0.18	0.03	0.21	1.85	0.05	0.15	0.02	0.14	0.03	0.53	37.49
LL-77	31.75	2.82	1.24	0.45	1.94	0.38	0.08	0.44	0.06	0.39	4.17	0.08	0.22	0.03	0.18	0.03	0.25	50.92
LL-78	32.40	5.28	6.20	1.05	4.41	0.77	0.15	0.80	0.11	0.67	5.41	0.14	0.35	0.04	0.28	0.04	0.60	39.64
LL-84	37.00	4.13	3.19	0.81	3.59	0.72	0.14	0.79	0.13	0.79	6.24	0.17	0.45	0.06	0.39	0.06	0.40	36.76
LL-87	40.80	5.92	4.70	1.30	5.52	1.06	0.24	1.17	0.19	1.20	8.60	0.26	0.68	0.10	0.59	0.09	0.39	33.48

注: Ce/Ce^{*}=2Ce_n/(La_n+Pr_n), “n”代表PAAS。

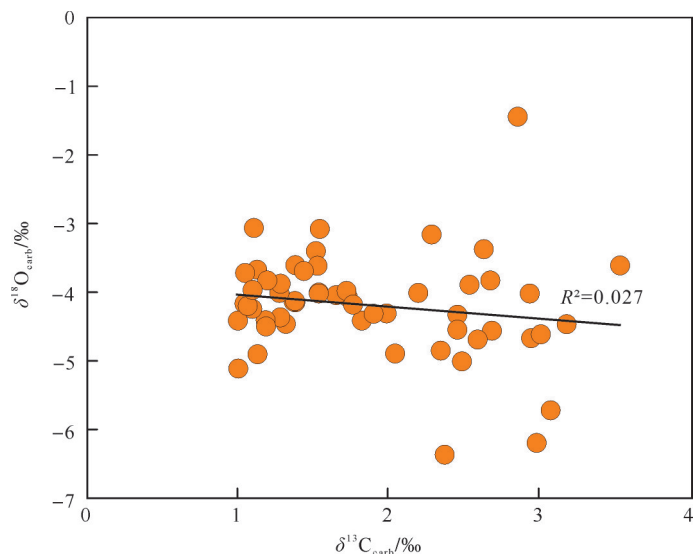


图4 拉利剖面碳酸盐岩 $\delta^{13}\text{C}_{\text{carb}}$ - $\delta^{18}\text{O}_{\text{carb}}$ 交会图
Fig.4 Cross plot of carbonate $\delta^{13}\text{C}_{\text{carb}}$ vs. $\delta^{18}\text{O}_{\text{carb}}$ at Lali section

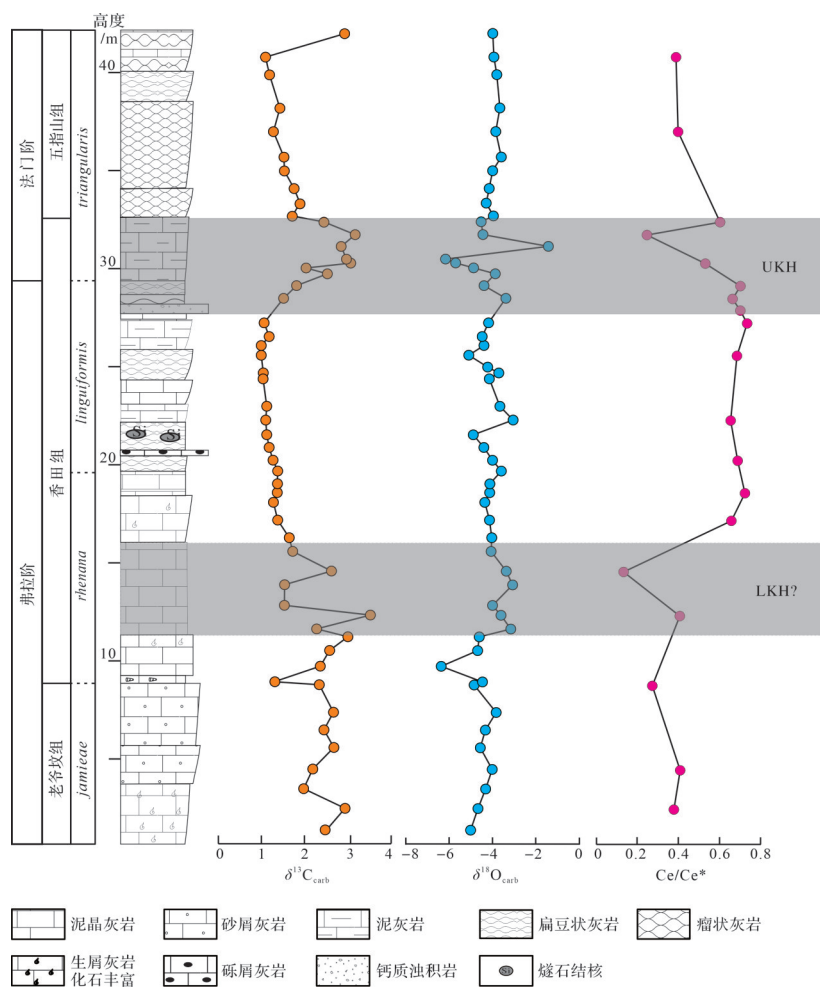


图5 拉利剖面灰岩 $\delta^{13}\text{C}_{\text{carb}}$ 、 $\delta^{18}\text{O}_{\text{carb}}$ 和 Ce/Ce^* 变化图
Fig.5 Profiles of $\delta^{13}\text{C}_{\text{carb}}$, $\delta^{18}\text{O}_{\text{carb}}$ and Ce/Ce^* at Lali section

灰岩、泥质灰岩段发生了明显增大(图5),由最小值0.13增长到最大值0.73,增幅达到0.60。因此,尽管拉利剖面碳酸盐岩 Ce/Ce^* 值总体呈负异常,但垂向差异较大,在F-F界线之下(UKH层及其之下)海水变得更加还原;而LKH层 Ce/Ce^* 较小,也没有明显的增大,表明LKH层并未发生明显的缺氧,类似于部分欧洲、北美剖面结果^[33,36]。

3.2.2 华南其他剖面氧化还原状态及缺氧模式

Zhang *et al.*^[46]曾通过氧化还原敏感元素对华南广西地区深水海槽相(与广海相连)的板城剖面(图6)进行了氧化还原状态研究,结果显示Mo、U和V元素在F-F界线附近没有富集,表明板城地区在UKH和LKH层及其附近沉积时海水没有出现缺氧,仍然保持氧化状态(图6)^[46]。

Cai *et al.*^[72]通过硫同位素和铁组分对华南近陆源的滨岸台地相的锡矿山剖面(图7)F-F转折期的缺氧

事件进行了研究。结果显示,UKH事件层, $\text{Fe}_{\text{HR}}/\text{Fe}_T$ 大于0.38, $\text{Fe}_{\text{Py}}/\text{Fe}_{\text{HR}}$ 升至0.88,有机硫(S_{Keno})和黄铁矿硫(S_{Py})同位素值大幅负偏, $\Delta^{34}\text{S}_{\text{Keno-Py}}$ 的快速减小(图7),海洋硫酸盐浓度大幅降低,表明海洋环境从氧化状态快速转变为缺氧硫化状态^[72]。

综上,从锡矿山、拉利和板城剖面的研究成果来看,最靠近陆源、水体最浅的锡矿山剖面缺氧程度最高,UKH层缺氧硫化;相对远离大陆、水体较浅的台地边缘—斜坡相拉利剖面UKH层及其之下相对还原;而更加开阔、更深水、更加远离大陆的板城剖面持续氧化。由此可见,在华南地区,“由上至下”的缺氧模式更为合理(图8)。此外,晚泥盆世华南地区呈网格状、台地—台间盆地间隔的古地理格局,且海平面在F-F之交整体呈下降趋势^[13,43],这在很大程度抑制了上升洋流,一定程度支持了大陆风化增强最终导致海水缺氧的模式。

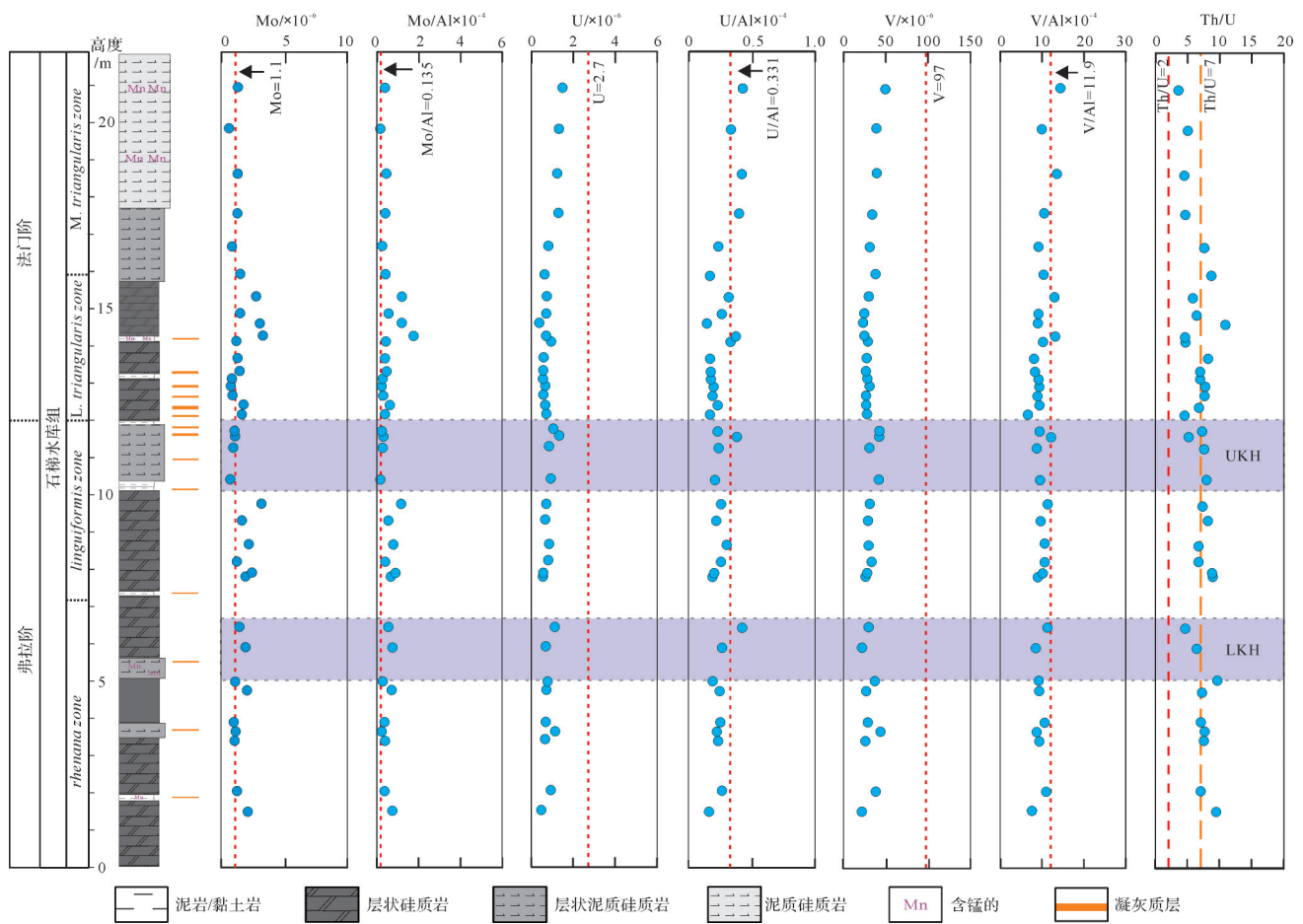


图6 板城剖面F-F转折期Mo, U, V含量及Mo/Al, U/Al, V/Al, Th/U元素比值垂向变化图(据文献[46]修改)

Fig.6 Stratigraphic distributions of Mo, U, V concentrations and Mo/Al, U/Al, V/Al, Th/U ratios at Bancheng section during F-F transition (modified from reference [46])

Carmichael *et al.*^[79]关于晚泥盆世孤立岛弧环境的缺氧研究显示,晚泥盆世开阔海中岛弧两侧水体出现短暂缺氧;然而上升流、水体停滞以及热液活动引起的缺氧(即上升流模型)都不能很好地解释岛弧两侧水体缺氧现象^[65]。此外,大量的研究证实该时期有明显的初级生产力增强以及透光带富营养化现象^[32,34,50,62,64,67],因此风化作用增强引起输入海洋的陆源营养物质增加,导致近陆源的陆缘海地区的海水富营养化和缺氧的模式受到了更多学者的青睐。

4 F-F生物危机的成因探讨

综上所述,F-F转折期,古气候、古海洋等环境要素发生了明显波动。各环境要素间存在一定的成因联系,它们对F-F转折期的生物演变有着不同程度的影响。

F-F转折期的气候变化与底栖生物为主的生物消亡有着较好的对应关系(图2),表明气候对于F-F

生物危机有着直接且深刻的影响。F-F转折期的缺氧事件的出现时间、程度在世界各地表现不一(图3),很难直接将海洋缺氧与F-F事件对应,缺氧程度、范围对于灭绝事件的影响需要进一步的明确和限定,但不能排除浅海的缺氧对F-F事件有一定的影响。

北非、欧洲等地的Kellwasser事件层发现了汞元素的异常富集^[9];西伯利亚Vilyu玄武岩(Vilyu Traps)、瑞典Sijan火山口、东欧台地强烈的裂谷火山活动、中亚造山带等地的岛弧岩浆作用以及华南的凝灰岩层均被视为F-F转折期火山作用的证据^[46,80]。频繁、短周期的火山放气作用会大幅增强大陆风化作用,一方面引起气候在变冷的趋势下多次暖—冷交替;另一方面可能向表层海水输入大量的营养物质,造成靠近陆源的浅海短暂富营养化和缺氧(图9)。世界各地表现不一的缺氧程度和范围也指示海水缺氧的诱因可能并不单一。气候与海洋环境的变化给热带浅海底栖生物造成极大的环境压力,使它

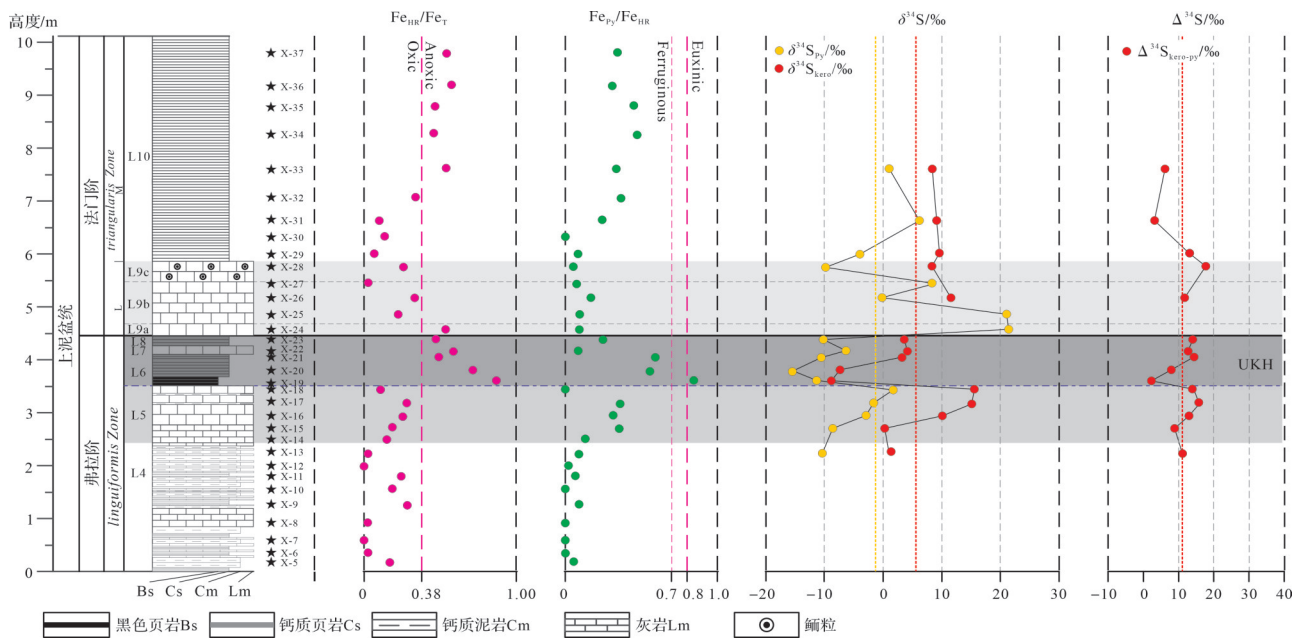


图7 锡矿山剖面F-F转折期铁组分($\text{Fe}_{\text{HR}}/\text{Fe}_T$, $\text{Fe}_{\text{Py}}/\text{Fe}_{\text{HR}}$)与硫同位素($\delta^{34}\text{S}_{\text{Kero}}$, $\delta^{34}\text{S}_{\text{Py}}$, $\delta^{34}\text{S}_{\text{Kero-Py}}$)垂向变化图
(据文献[72]修改)

Fig.7 Stratigraphic distributions of Fe speciation ($\text{Fe}_{\text{HR}}/\text{Fe}_T$, $\text{Fe}_{\text{Py}}/\text{Fe}_{\text{HR}}$) and sulfur isotopes ($\delta^{34}\text{S}_{\text{Kero}}$, $\delta^{34}\text{S}_{\text{Py}}$, $\delta^{34}\text{S}_{\text{Kero-Py}}$) at Xikuangshan during F-F transition (modified from reference [72])

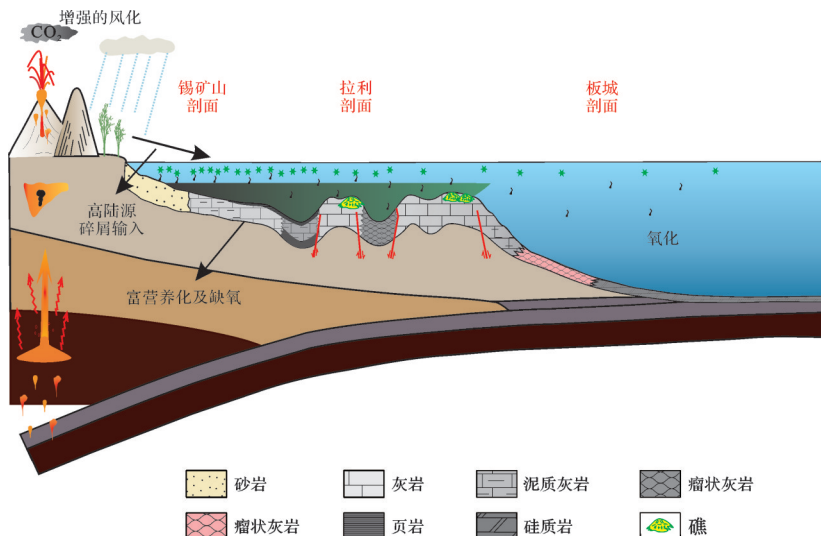


图8 华南F-F转折海水氧化还原状态模式图(据文献[46]修改)

Fig.8 Schematic diagram of marine redox states in southern China during F-F transition (modified from reference [46])

们生理上难以适应,大量消亡。因此F-F生物危机并不是单一环境因素造成的,而是由火山构造活动、气候、海洋环境(海平面、氧化还原状态等)等因素相互作用,相互反馈最终导致(图9)。

5 结论

F-F转折期,气候整体变冷,期间存在多次暖—

冷交替;海洋缺氧主要集中在靠近陆源的浅海,缺氧范围和程度各地表现不一,可能是增强的大陆风化作用导致。火山活动,特别是陆弧火山幕式作用可能是引起气候波动,海洋环境变化的内生触发因素。因此,F-F生物危机更可能是多种环境因素相互作用、互相反馈共同导致,而非单一因素引起。

致谢 感谢中国科学院地质与地球物理研究所李文君高级工程师和崔琳琳高级工程师在实验分析

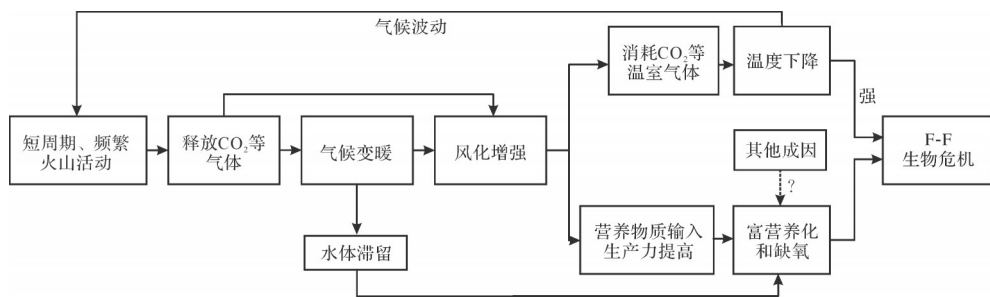


图9 F-F转折期各环境要素因果关系图

Fig.9 Flowchart of cause-and-effect among environmental factors during F-F transition

过程中给予的帮助，感谢审稿专家及编辑在审稿、排版和校对过程中提出的宝贵修改意见。

参考文献(References)

- [1] Algeo T J, Berner R A, Maynard J B, et al. Late Devonian oceanic anoxic events and biotic crises: “rooted” in the evolution of vascular land plants? [J]. *GSA Today*, 1995, 5(3): 63-66.
- [2] van Geldern R, Joachimski M M, Day J, et al. Carbon, oxygen and strontium isotope records of Devonian brachiopod shell calcite [J]. *Palaeogeography, Palaeoclimatology, Palaeoecology*, 2006, 240(1/2): 47-67.
- [3] Percival L M E, Selby D, Bond D P G, et al. Pulses of enhanced continental weathering associated with multiple Late Devonian climate perturbations: Evidence from osmium-isotope compositions[J]. *Palaeogeography, Palaeoclimatology, Palaeoecology*, 2019, 524: 240-249.
- [4] Streel M, Caputo M V, Loboziak S, et al. Late Frasnian–Famennian climates based on palynomorph analyses and the question of the Late Devonian glaciations[J]. *Earth-Science Reviews*, 2000, 52(1/2/3): 121-173.
- [5] Joachimski M M, van Geldern R, Breisig S, et al. Oxygen isotope evolution of biogenic calcite and apatite during the Middle and Late Devonian[J]. *International Journal of Earth Sciences*, 2004, 93(4): 542-553.
- [6] Joachimski M M, Breisig S, Buggisch W, et al. Devonian climate and reef evolution: Insights from oxygen isotopes in apatite[J]. *Earth and Planetary Science Letters*, 2009, 284(3/4): 599-609.
- [7] Over D J. The Frasnian/Famennian boundary in central and eastern United States[J]. *Palaeogeography, Palaeoclimatology, Palaeoecology*, 2002, 181(1/2/3): 153-169.
- [8] Chen D Z, Qing H R, Li R W. The Late Devonian Frasnian–Famennian (F/F) biotic crisis: Insights from $\delta^{13}\text{C}_{\text{carb}}$, $\delta^{13}\text{C}_{\text{org}}$ and $^{87}\text{Sr}/^{86}\text{Sr}$ isotopic systematics[J]. *Earth and Planetary Science Letters*, 2005, 235(1/2): 151-166.
- [9] Racki G, Rakociński M, Marynowski L, et al. Mercury enrichments and the Frasnian-Famennian biotic crisis: A volcanic trigger proved? [J]. *Geology*, 2018, 46(6): 543-546.
- [10] McGhee G R, Jr. The Late Devonian mass extinction: The Frasnian/Famennian crisis[M]. New York: Columbia University Press, 1996.
- [11] Racki G. Frasnian–Famennian biotic crisis: Undervalued tectonic control? [J]. *Palaeogeography, Palaeoclimatology, Palaeoecology*, 1998, 141(3/4): 177-198.
- [12] Sandberg C A, Morrow J R, Ziegler W. Late Devonian sea-level changes, catastrophic events, and mass extinctions[M]//Koeberl C, MacLeod K G. Catastrophic events and mass extinctions: Impacts and beyond. Boulder: Geological Society of America, 2002: 473-488.
- [13] Chen D Z, Tucker M E. The Frasnian–Famennian mass extinction: Insights from high-resolution sequence stratigraphy and cyclostratigraphy in South China[J]. *Palaeogeography, Palaeoclimatology, Palaeoecology*, 2003, 193(1): 87-111.
- [14] Kaiser S I, Aretz M, Becker R T. The global Hangenberg Crisis (Devonian – Carboniferous transition): Review of a first-order mass extinction[J]. *Geological Society, London, Special Publications*, 2016, 423(1): 387-437.
- [15] 戎嘉余, 黄冰. 生物大灭绝研究三十年[J]. 中国科学(D辑): 地球科学, 2014, 44(3): 377-404. [Rong Jiayu, Huang Bing. Study of Mass Extinction over the past thirty years: A synopsis [J]. *Science China (Ser. D): Earth Sciences*, 2014, 44(3): 377-404.]
- [16] Whiteside J H, Grice K. Biomarker records associated with mass extinction events[J]. *Annual Review of Earth and Planetary Sciences*, 2016, 44: 581-612.
- [17] Erlykin A D, Harper D A T, Sloan T, et al. Mass extinctions over the last 500 myr: An astronomical cause? [J]. *Palaeontology*, 2017, 60(2): 159-167.
- [18] 沈树忠, 张华. 什么引起五次生物大灭绝? [J]. 科学通报, 2017, 62(11): 1119-1135. [Shen Shuzhong, Zhang Hua. What caused the five mass extinctions? [J]. *Chinese Science Bulletin*, 2017, 62(11): 1119-1135.]
- [19] Copper P. Reef development at the Frasnian/Famennian mass extinction boundary[J]. *Palaeogeography, Palaeoclimatology, Palaeoecology*, 2002, 181(1/2/3): 27-65.
- [20] Olempska E. The Late Devonian Upper Kellwasser Event and entomozoacean ostracods in the Holy Cross Mountains, Poland [J]. *Acta Palaeontologica Polonica*, 2002, 47(2): 247-266.

- [21] Ma X P, Gong Y M, Chen D Z, et al. The Late Devonian Frasnian-Famennian Event in South China: Patterns and causes of extinctions, sea level changes, and isotope variations [J]. *Palaeogeography, Palaeoclimatology, Palaeoecology*, 2016, 448: 224-244.
- [22] Sorauf J E, Pedder A E H. Late Devonian rugose corals and the Frasnian-Famennian crisis[J]. *Canadian Journal of Earth Sciences*, 1986, 23(9): 1265-1287.
- [23] 廖卫华. 华南中泥盆世两次重要的珊瑚群更替事件[J]. 古生物学报, 2015, 54 (3) : 305-315. [Liao Weihua. Two major faunal turnover events of Middle Devonian corals in South China [J]. *Acta Palaeontologica Sinica*, 2015, 54(3): 305-315.]
- [24] 董俊彦, 龚一鸣. 层孔虫研究进展与展望[J]. 古地理学报, 2019, 21(5) : 783-802. [Dong Junyan, Gong Yiming. Progress and prospects of studies on stromatoporoids[J]. *Journal of Palaeogeography*, 2019, 21(5): 783-802.]
- [25] 王玉珏, 梁昆, 陈波, 等. 晚泥盆世F-F大灭绝事件研究进展 [J]. 地层学杂志, 2020, 44(3) : 277-298. [Wang Yujue, Liang Kun, Chen Bo, et al. Research progress in the Late Devonian F-F mass extinction[J]. *Journal of Stratigraphy*, 2020, 44(3): 277-298.]
- [26] 宋俊俊, 龚一鸣. 古生代介形类的研究现状及展望[J]. 古生物学报, 2015, 54(3) : 404-424. [Song Junjun, Gong Yiming. Progresses and prospects of palaeozoic ostracod study[J]. *Acta Palaeontologica Sinica*, 2015, 54(3): 404-424.]
- [27] Huang C, Joachimski M M, Gong Y M. Did climate changes trigger the Late Devonian Kellwasser Crisis? Evidence from a high-resolution conodont $\delta^{18}\text{O}_{\text{PO}_4}$ record from South China[J]. *Earth and Planetary Science Letters*, 2018, 495: 174-184.
- [28] Li Y X. Famennian tentaculitids of China[J]. *Journal of Paleontology*, 2000, 74(5): 969-975.
- [29] Becker R T. Anoxia, eustatic changes, and Upper Devonian to lowermost Carboniferous global ammonoid diversity[M]//House M R. The ammonioidea: Environment, ecology, and evolutionary change. Oxford: Clarendon Press, 1993, 47: 115-163.
- [30] Johnson J G, Klapper G, Sandberg C A. Devonian eustatic fluctuations in Euramerica[J]. *GSA Bulletin*, 1985, 96(5): 567-587.
- [31] Bond D P G, Wignall P B. The role of sea-level change and marine anoxia in the Frasnian–Famennian (Late Devonian) mass extinction[J]. *Palaeogeography, Palaeoclimatology, Palaeoecology*, 2008, 263(3/4): 107-118.
- [32] Murphy A E, Sageman B B, Hollander D J. Eutrophication by decoupling of the marine biogeochemical cycles of C, N, and P: A mechanism for the Late Devonian mass extinction[J]. *Geology*, 2000, 28(5): 427-430.
- [33] Bond D, Wignall P B, Racki G. Extent and duration of marine anoxia during the Frasnian–Famennian (Late Devonian) mass extinction in Poland, Germany, Austria and France[J]. *Geological Magazine*, 2004, 141(2): 173-193.
- [34] Marynowski L, Rakociński M, Borcuch E, et al. Molecular and petrographic indicators of redox conditions and bacterial communities after the F/F mass extinction (Kowala, Holy Cross Mountains, Poland)[J]. *Palaeogeography, Palaeoclimatology, Palaeoecology*, 2011, 306(1/2): 1-14.
- [35] Whalen M T, Śliwiński M G, Payne J H, et al. Chemostratigraphy and magnetic susceptibility of the Late Devonian Frasnian–Famennian transition in western Canada and southern China: Implications for carbon and nutrient cycling and mass extinction [J]. *Geological Society, London, Special Publications*, 2015, 414 (1): 37-72.
- [36] White D A, Elrick M, Romaniello S, et al. Global seawater redox trends during the Late Devonian mass extinction detected using U isotopes of marine limestones[J]. *Earth and Planetary Science Letters*, 2018, 503: 68-77.
- [37] Joachimski M M, Buggisch W. Conodont apatite $\delta^{18}\text{O}$ signatures indicate climatic cooling as a trigger of the Late Devonian mass extinction[J]. *Geology*, 2002, 30(8): 711-714.
- [38] Zhang L Y, Chen D Z, Huang T Y, et al. An abrupt oceanic change and frequent climate fluctuations across the Frasnian–Famennian transition of Late Devonian: Constraints from conodont Sr isotope[J]. *Geological Journal*, 2020, 55(6): 4479-4492.
- [39] Wang K, Orth C J, Attrep M, Jr, et al. Geochemical evidence for a catastrophic biotic event at the Frasnian/Famennian boundary in South China[J]. *Geology*, 1991, 19(8): 776-779.
- [40] Golonka J. Phanerozoic palaeoenvironment and palaeolithofacies maps of the Arctic region[J]. *Geological Society, London, Memoirs*, 2011, 35(1): 79-129.
- [41] Thompson J B, Newton C R. Late Devonian mass extinction: Episodic climatic cooling or warming? [M]//McMillan N J, Embry A F, Glass D J. Devonian of the world. Calgary: Canadian Society of Petroleum Geologists, 1988: 29-34.
- [42] Hallam A, Wignall P B. Mass extinctions and sea-level changes [J]. *Earth-Science Reviews*, 1999, 48(4): 217-250.
- [43] Chen D Z, Tucker M. Palaeokarst and its implication for the extinction event at the Frasnian–Famennian boundary (Guilin, South China) [J]. *Journal of the Geological Society*, 2004, 161 (6): 895-898.
- [44] Le Houedec S, Girard C, Balter V. Conodont Sr/Ca and $\delta^{18}\text{O}$ record seawater changes at the Frasnian–Famennian boundary[J]. *Palaeogeography, Palaeoclimatology, Palaeoecology*, 2013, 376: 114-121.
- [45] Gereke M, Schindler E. “Time-Specific Facies” and biological crises: The Kellwasser Event interval near the Frasnian/Famennian boundary (Late Devonian) [J]. *Palaeogeography, Palaeoclimatology, Palaeoecology*, 2012, 367-368: 19-29.
- [46] Zhang L Y, Chen D Z, Kuang G D, et al. Persistent oxic deep ocean conditions and frequent volcanic activities during the Frasnian–Famennian transition recorded in South China[J]. *Global and Planetary Change*, 2020, 195: 103350.

- [47] Zhang X S, Joachimski M M, Gong Y M. Late Devonian greenhouse-icehouse climate transition: New evidence from conodont $\delta^{18}\text{O}$ thermometry in the eastern Palaeotethys (Lali section, South China)[J]. *Chemical Geology*, 2021, 581: 120383.
- [48] Joachimski M M, Pancost R D, Freeman K H, et al. Carbon isotope geochemistry of the Frasnian-Famennian transition[J]. *Palaeogeography, Palaeoclimatology, Palaeoecology*, 2002, 181 (1/2/3): 91-109.
- [49] Chang J Q, Bai Z Q, Sun Y L, et al. High resolution bio- and chemostratigraphic framework at the Frasnian-Famennian boundary: Implications for regional stratigraphic correlation between different sedimentary facies in South China[J]. *Palaeogeography, Palaeoclimatology, Palaeoecology*, 2019, 531: 108299.
- [50] Gong Y M, Xu R, Tang Z D, et al. Relationships between bacterial-algal proliferating and mass extinction in the Late Devonian Frasnian-Famennian transition: Enlightening from carbon isotopes and molecular fossils[J]. *Science in China Series D: Earth Sciences*, 2005, 48(10): 1656-1665.
- [51] Simon L, Goddérat Y, Buggisch W, et al. Modeling the carbon and sulfur isotope compositions of marine sediments: Climate evolution during the Devonian[J]. *Chemical Geology*, 2007, 246 (1/2): 19-38.
- [52] Hayes J M, Strauss H, Kaufman A J. The abundance of ^{13}C in marine organic matter and isotopic fractionation in the global biogeochemical cycle of carbon during the past 800 Ma[J]. *Chemical Geology*, 1999, 161(1/2/3): 103-125.
- [53] Kump L R, Arthur M A. Interpreting carbon-isotope excursions: Carbonates and organic matter[J]. *Chemical Geology*, 1999, 161 (1/2/3): 181-198.
- [54] 陈代钊,王卓卓,汪建国. 晚泥盆世地球各圈层相互作用与海洋生态危机:来自高分辨率的沉积和同位素地球化学证据[J]. *自然科学进展*, 2006, 16(4): 439-448. [Chen Daizhao, Wang Zhuozhuo, Wang Jianguo. Earth's sphere interactions and marine ecological crisis in the Late Devonian: High-resolution sedimentary and isotopic geochemical evidence[J]. *Progress in Natural Science*, 2006, 16(4): 439-448.]
- [55] Veizer J, Buhl D, Diener A, et al. Strontium isotope stratigraphy: Potential resolution and event correlation[J]. *Palaeogeography, Palaeoclimatology, Palaeoecology*, 1997, 132(1/2/3/4): 65-77.
- [56] Jones C E, Jenkyns H C. Seawater strontium isotopes, oceanic anoxic events, and seafloor hydrothermal activity in the Jurassic and Cretaceous[J]. *American Journal of Science*, 2001, 301(2): 112-149.
- [57] Averbuch O, Tribouillard N, Devleeschouwer X, et al. Mountain building-enhanced continental weathering and organic carbon burial as major causes for climatic cooling at the Frasnian-Famennian boundary (*c.* 376 Ma)?[J]. *Terra Nova*, 2005, 17(1): 25-34.
- [58] Algeo T J, Scheckler S E. Land plant evolution and weathering rate changes in the Devonian[J]. *Journal of Earth Science*, 2010, 21(Suppl. 1): 75-78.
- [59] Joachimski M M, Buggisch W. Anoxic events in the Late Frasnian: Causes of the Frasnian-Famennian faunal crisis?[J]. *Geology*, 1993, 21(8): 675-678.
- [60] Riquier L, Tribouillard N, Averbuch O, et al. The Late Frasnian Kellwasser horizons of the Harz Mountains (Germany): Two oxygen-deficient periods resulting from different mechanisms [J]. *Chemical Geology*, 2006, 233(1/2): 137-155.
- [61] Bond D, Wignall P B. Evidence for Late Devonian (Kellwasser) anoxic events in the Great Basin, western United States[J]. *Developments in Palaeontology and Stratigraphy*, 2005, 20: 225-262.
- [62] Haddad E E, Boyer D L, Droser M L, et al. Ichnofabrics and chemostratigraphy argue against persistent anoxia during the Upper Kellwasser Event in New York State[J]. *Palaeogeography, Palaeoclimatology, Palaeoecology*, 2018, 490: 178-190.
- [63] Sim M S, Ono S, Hurtgen M T. Sulfur isotope evidence for low and fluctuating sulfate levels in the Late Devonian ocean and the potential link with the mass extinction event[J]. *Earth and Planetary Science Letters*, 2015, 419: 52-62.
- [64] Joachimski M M, Ostertag-Henning C, Pancost R D, et al. Water column anoxia, enhanced productivity and concomitant changes in $\delta^{13}\text{C}$ and $\delta^{34}\text{S}$ across the Frasnian-Famennian boundary (Kowala—Holy Cross Mountains/Poland)[J]. *Chemical Geology*, 2001, 175(1/2): 109-131.
- [65] Carmichael S K, Waters J A, Königshof P, et al. Paleogeography and paleoenvironments of the Late Devonian Kellwasser Event: A review of its sedimentological and geochemical expression[J]. *Global and Planetary Change*, 2019, 183: 102984.
- [66] John E H, Wignall P B, Newton R J, et al. $\delta^{34}\text{S}_{\text{CAS}}$ and $\delta^{18}\text{O}_{\text{CAS}}$ records during the Frasnian–Famennian (Late Devonian) transition and their bearing on mass extinction models[J]. *Chemical Geology*, 2010, 275(3/4): 221-234.
- [67] George A D, Chow N, Trinajstic K M. Oxic facies and the Late Devonian mass extinction, Canning Basin, Australia[J]. *Geology*, 2014, 42(4): 327-330.
- [68] Tissot F L H, Dauphas N. Uranium isotopic compositions of the crust and ocean: Age corrections, U budget and global extent of modern anoxia[J]. *Geochimica et Cosmochimica Acta*, 2015, 167: 113-143.
- [69] Lau K V, Macdonald F A, Maher K, et al. Uranium isotope evidence for temporary ocean oxygenation in the aftermath of the Sturtian Snowball Earth[J]. *Earth and Planetary Science Letters*, 2017, 458: 282-292.
- [70] Clarkson M O, Stirling C H, Jenkyns H C, et al. Uranium isotope evidence for two episodes of deoxygenation during Oceanic Anoxic Event 2[J]. *Proceedings of the National Academy of Sciences of the United States of America*, 2018, 115(12): 2918-2923.

- [71] Song H Y, Song H J, Algeo T J, et al. Uranium and carbon isotopes document global-ocean redox-productivity relationships linked to cooling during the Frasnian-Famennian mass extinction [J]. Geology, 2017, 45(10): 887-890.
- [72] Cai C F, Xu C L, Fakhraee M, et al. Significant fluctuation in the global sulfate reservoir and oceanic redox state during the Late Devonian event[J]. PNAS Nexus, 2022, 1(4): pgac122.
- [73] Kazmierczak J, Kremer B, Racki G. Late Devonian marine anoxia challenged by benthic cyanobacterial mats[J]. Geobiology, 2012, 10(5): 371-383.
- [74] Zhao Y Y, Zheng Y F, Chen F K. Trace element and strontium isotope constraints on sedimentary environment of Ediacaran carbonates in southern Anhui, South China[J]. Chemical Geology, 2009, 265(3/4): 345-362.
- [75] 常华进, 储雪蕾, 冯连君, 等. 氧化还原敏感微量元素对古海洋沉积环境的指示意义[J]. 地质论评, 2009, 55(1): 91-99.
[Chang Huajin, Chu Xuelei, Feng Lianjun, et al. Redox sensitive trace elements as paleoenvironments proxies[J]. Geological Review, 2009, 55(1): 91-99.]
- [76] Jacobsen S B, Kaufman A J. The Sr, C and O isotopic evolution of Neoproterozoic seawater[J]. Chemical Geology, 1999, 161(1/2/3): 37-57.
- [77] Tanaka K, Tani Y, Takahashi Y, et al. A specific Ce oxidation process during sorption of rare earth elements on biogenic Mn oxide produced by *Acremonium* sp. strain KR21-2[J]. Geochimica et Cosmochimica Acta, 2010, 74(19): 5463-5477.
- [78] Ling H F, Chen X, Li D, et al. Cerium anomaly variations in Ediacaran-earliest Cambrian carbonates from the Yangtze Gorges area, South China: Implications for oxygenation of coeval shallow seawater[J]. Precambrian Research, 2013, 225: 110-127.
- [79] Carmichael S K, Waters J A, Suttner T J, et al. A new model for the Kellwasser Anoxia Events (Late Devonian): Shallow water anoxia in an open oceanic setting in the Central Asian Orogenic Belt[J]. Palaeogeography, Palaeoclimatology, Palaeoecology, 2014, 399: 394-403.
- [80] Percival L M E, Davies J H F L, Schaltegger U, et al. Precisely dating the Frasnian-Famennian boundary: Implications for the cause of the Late Devonian mass extinction[J]. Scientific Report, 2018, 8(1): 9578.

Paleoclimatic and Paleo-Oceanic Environment Evolution in the Frasnian-Famennian Transition: Potential causes of the biotic crisis

ZHANG LiYu^{1,2}, CHEN DaiZhao³, LIU Kang⁴

1. Wuxi Research Institute of Petroleum Geology, Petroleum Exploration and Production Research Institute, SINOPEC, Wuxi, Jiangsu 214126, China

2. SINOPEC Key Laboratory of Petroleum Accumulation Mechanisms, Wuxi, Jiangsu 214126, China

3. Key Laboratory of Cenozoic Geology and Environment, Institute of Geology and Geophysics, Chinese Academy of Sciences, Beijing 100029, China

4. Key Laboratory of Petroleum Geochemistry, Research Institute of Petroleum Exploration and Development, CNPC, Beijing 100083, China

Abstract: [Objective] The Late Devonian Frasnian-Famennian (F-F) transition is a critical time interval in geological history. This period saw major simultaneous marine ecological system changes that led to one of the Big Five mass extinctions in the Phanerozoic. The F-F event (also referred to as the Kellwasser event) was characterized by severe losses of low-latitude shallow-water benthic faunas, notably reef-dwelling coral and stromatoporoids. High-latitude, deep-sea and terrestrial faunas were the least affected. Various separate or combined hypotheses have been proposed as the causes of this mass extinction (sea-level change, marine anoxia, climate change, volcanic/hydrothermal activities, and bolide impact). Of these, climate change and marine anoxia have been the most intensively researched and discussed hypotheses based on the Web of Science in recent years. However, some controversies remain, and the interactions of certain factors are still unclear. [Methods] This study systematically reviews available reports on the paleoclimatic and paleo-oceanic changes during the F-F transition and discusses the anoxic model during this critical period, based on related case studies in southern China. [Results and Conclusions] Conodont oxygen and strontium isotopes, as well as the carbon isotope records for carbonates, collectively suggest a cold climate during the F-F transition interval, with several rapid warming-cooling fluctuations. Conodont oxygen isotopes suggest that the sea-surface temperature (SST) dropped by 5 °C-8 °C. Strontium isotopes also imply that the temperature fluctuations were due to frequent, short-duration volcanism. Palynological data and carbonate platform exposure/karstification are also suggestive of coeval climate cooling. Additionally, marine anoxia has been extensively hypothesized as a possible killing mechanism in the F-F mass extinction, based initially on the presence of bituminous limestones (or black shales), named the lower and upper Kellwasser horizons. Studies of pyrite framboids, biomarker compounds, trace elements, isotopes of nitrogen, sulfur and uranium, and iron speciation have variously suggested the existence of the Kellwasser anoxic events. However, these generally occurred in geographically specific environments, notably in the pericontinental basins/sub-basins proximal to source hinterlands. Moreover, the range and degree of anoxia in the F-F transition also reportedly differed between study sections around the world. With regard to the anoxic model, studies have suggested that the Kellwasser anoxic events were caused by the increased nutrient input related to enhanced continental weathering. Marine anoxic studies from three F-F sections comprising different depositional facies in southern China also support this “top down” anoxic model. Clearly, the F-F biotic crisis was not caused by any single factor. Frequent short-term volcanic activity may have enhanced continental weathering and associated greenhouse gas emission, leading to frequent warming-cooling climate fluctuations and also increased oceanic nutrient input. In the latter case, eutrophication and anoxia would have occurred in shallow water, and the mutual interaction of the various environmental factors may have exerted biological pressure in the low-latitude shallow sea, and eventually led to the F-F biotic crisis.

Key words: Frasnian-Famennian transition; paleoclimate; paleo-oceanic redox condition; biotic crisis